

1408
X-651-73-67

PREPRINT

NASA TM X-66192

**THE MEAN OZONE DISTRIBUTION FROM
SEVERAL SERIES OF ROCKET SOUNDINGS
TO 52 KM AT LATITUDES FROM
58° S TO 64° N**

ARLIN J. KRUEGER

(NASA-TM-X-66192) THE MEAN OZONE
DISTRIBUTION FROM SEVERAL SERIES OF
ROCKET SOUNDING TO 52 km AT LATITUDES
FROM 58 DEG S TO 64 DEG N (NASA) 17 p
HC \$3.00

N73-18391

CSCL 04A G3/13 Unclass 63938

FEBRUARY 1973

GSFC

**GODDARD SPACE FLIGHT CENTER
GREENBELT, MARYLAND**

THE MEAN OZONE DISTRIBUTION FROM SEVERAL
SERIES OF ROCKET SOUNDINGS TO
52 KM AT LATITUDES FROM 58° S TO 64° N

Arlin J. Krueger
Meteorology Branch

February 1973

GODDARD SPACE FLIGHT CENTER
Greenbelt, Maryland

PRECEDING PAGE BLANK NOT FILMED

THE MEAN OZONE DISTRIBUTION FROM SEVERAL
SERIES OF ROCKET SOUNDINGS TO 52 km
AT LATITUDES FROM 58° S TO 64° N

Arlin J. Krueger
Meteorology Branch

ABSTRACT

The results of 21 rocket flights of Arcas optical ozone-sondes have been combined to produce estimates of the mean ozone distribution and its variability; these estimates apply to a broad range of latitudes. The flights were launched from sites near the equator to 58° S and to 64° N, in the years from 1965 to 1971. The local-noon mean ozone densities in molecules/cubic centimeter are 7.0×10^{10} at 50 km, 6.7×10^{11} at 40 km, 3.1×10^{12} at 30 km, and 3.1×10^{12} at 20 km. The maximum density is 4.5×10^{12} at 24 km. The range of observed densities is about ± 30 percent of the mean value at 50 km; ± 40 percent at 40 km; ± 40 percent at 30 km; and +200 percent, -66 percent at 20 km. The variabilities in this set of observations are much smaller than those indicated by previous measurements.

Preceding page blank

PRECEDING PAGES BLANK NOT FILMED

CONTENTS

	<u>Page</u>
INTRODUCTION	1
CHARACTERISTICS OF DIRECT OPTICAL OZONE-SOUNDING TECHNIQUES	1
ROCKET INSTRUMENT CHARACTERISTICS	2
ACCURACIES	3
ROCKET FLIGHT SUMMARY	4
Mean Ozone Densities	6
Variabilities	11
ACKNOWLEDGEMENTS	11
REFERENCES	12

Preceding page blank

THE MEAN OZONE DISTRIBUTION FROM SEVERAL SERIES OF ROCKET SOUNDINGS TO 52 km AT LATITUDES FROM 58° S TO 64° N

INTRODUCTION

Since 1965, several series of rocket flights have been made to measure the distribution of ozone to about 50 km, using an optical ozonesonde in which special care was taken to avoid sources of biases. At the present time, results have been obtained from total of 27 flights at diverse locations from the equator to about 60° latitude in both hemispheres. About two-thirds of the flights were made for special purposes, such as for comparison with satellite-borne ozone-sensing instruments. The remaining flights were made to assess latitude gradients in the high-level ozone and to determine ozone changes during special geophysical situations.

The body of data collected in these flights provides a base for estimation of the general character of the ozone distribution under a broad range of latitude and seasonal conditions. In this study, data from 21 soundings are statistically analyzed for the mean ozone densities and variabilities for altitudes from 20 to 52 km.

CHARACTERISTICS OF DIRECT OPTICAL OZONE-SOUNDING TECHNIQUES

Absorption spectrometric techniques have been utilized for the direct determination of the vertical distribution of stratospheric ozone since the earliest exploratory work in this area. Because of the intensity of the Hartley absorption band of ozone, sunlight at wavelengths between 2300 and 2800 Angstroms is completely absorbed at altitudes above 30 km. Only in the Huggens bands, at wavelengths longer than approximately 2950 Angstroms, can the light penetrate to the bottom of the atmosphere. By measurement of the change in light intensity with height at one or more wavelengths in the Hartley and Huggens bands, it is possible to determine the vertical ozone distribution. The earliest application of this technique was by Regener and Regener (Reference 1), who obtained a series of photographic spectra of the sun from an ascending balloon. The height range was subsequently expanded to cover the entire stratosphere and lower mesosphere by Johnson et al. (Reference 2), who conducted similar measurements from an Aerobee rocket. The ozone distribution from that flight, launched on June 14, 1949, at White Sands Missile Range, has been rather widely accepted as representing photochemical equilibrium ozone concentrations, although corrections for revised ozone absorption coefficients have been necessary (Reference 3).

The optical technique was later adapted for routine soundings on balloons by Kulcke and Paetzold (Reference 4), Vassy (Reference 5), and Kobayashi, Kyojuka, and Muramatsu (Reference 6). By using filter-photometric methods, they were able to reduce the cost and complexity of the instrumentation and to standardize the data processing. For the altitudes normally accessible to balloons (0-30 km), measurements at a single wavelength channel in the Huggens bands are sufficient, although a second reference channel at longer, unabsorbed wavelengths is normally used to compensate for instrument changes.

Some of the first information on the latitudinal variations of the vertical ozone distribution came during the International Geophysical Year, from balloon flights of these instruments. More recently, direct-sampling chemical ozone-sondes have been generally used on balloons because the optical techniques are incapable of high vertical resolution at altitudes below the ozone maximum (25 km). At these levels, the total amount of ozone overhead is large and the local ozone concentrations are relatively low, thus leading to small changes in light intensity with height. This problem is compounded by atmospherically scattered light, which is a significant fraction of the light intensity measured by the optical sondes at altitudes below 20 km. A more favorable situation is found at levels above the ozone density maximum. There, the ozone overburden decreases almost exponentially with increasing height and the density at each level is 10 to 20 percent of the amount of ozone overhead. Under these conditions the vertical gradient of light intensity is large and results of good accuracy and resolution are possible.

ROCKET INSTRUMENT CHARACTERISTICS

Beginning in the early 1960s, a filter-photometer instrument employing several optical balloonsonde principles was designed for parachute dropsonde use with the Arcas meteorological sounding rocket (Reference 7). While a single active wavelength channel was sufficient at balloon altitudes, at least one additional channel at a shorter wavelength with a correspondingly higher ozone absorption coefficient is required for measurements to 55 km. However, by the use of two additional channels, redundant information is available in two height regions where channels adjacent in wavelength produce results of comparable accuracy. The latter approach was selected because the natural variability of ozone above 30 km was largely unknown and because the redundant data could serve to assess whether biases might exist in the computed ozone densities. The wavelengths of the three active channels are presently set near 3000, 2875, and 2650 Angstroms, so that the ozone absorption coefficients are related by the ratios 1:5:20. This selection of wavelengths results

in redundant ozone data for regions four to six km in altitude centered near 34 and 42 km, and still allows for useful measurements over a nearly hundred-fold dynamic range in ozone concentrations. A fourth, reference channel is centered near 3200 Angstroms, where the ozone absorption coefficient is only about 5 percent of the value at 3000 Angstroms.

ACCURACIES

The data accuracies attained by this system depend principally on three parameters: absorption-coefficient errors, photometer and telemetry errors, and optical sampling errors.

The absorption-coefficient errors determine the absolute accuracy of the ozone densities computed from each of the channels, while the other error sources determine the precision (or height-resolution capability). Because the optical channels are defined by interference filters, usually with 40 Angstroms widths at the half-peak transmission points, it is necessary to compute effective absorption coefficients for each channel (Reference 7). Errors in these effective absorption coefficients (which are functions of the slant-path ozone amount and, to a lesser degree, the overhead air mass) arise primarily from inaccuracies in spectral-transmission data for the long-wavelength wing of the filter. Unless these transmission values have very large errors (~100 percent), the accuracy of the effective absorption coefficients for small ozone optical depths should be close to the accuracies of the ozone absorption coefficients. These values, taken from Inn and Tanaka (Reference 8) for wavelengths less than 3000 Angstroms and from Vigroux (Reference 9) for longer wavelengths, appear to be of better than 5 percent accuracy.

Because of the redundant data available from the three channels in the rocket flights, it has been possible to test for consistency in the effective absorption coefficients. It is found that, with good control of the filter-transmission data in the long-wavelength wings of the filters, agreement between channels within 20 percent is possible for optical depths less than two. However, such agreement is rarely possible for much greater optical depths. In cases where significant disagreements are found for the smaller optical depths, reevaluation of the filter-transmission data is necessary.

In the present system, the photometric and telemetry errors affect the precision of the ozone-density determination. Instrumental factors, such as sensitivity changes, are cancelled by the use of ratios between signals from active and reference channels. The noise levels found in past flights lead to 10 to 20 percent uncertainties in the ozone concentrations for a height resolution of 1 km.

The optical sampling errors also tend to be random. However, biases can arise from intermodulation between the channel-sampling rate and the parachute pendulation and instrument rotation rates if the instrument response is dependent on the angle of illumination. In the few cases where these errors are suspected, somewhat periodic modulations over three- to four-kilometer height regions with amplitudes less than 10 percent of the mean ozone density have been found.

ROCKET FLIGHT SUMMARY

Since operational flights of the Arcas ozonesonde were begun in 1965, ozone distributions have been obtained on 27 flights. The initial soundings were made with the NASA-sponsored Mobile Launch Expedition. Five ozone distributions, obtained at latitudes from 4° N to 58° S during this cruise along the west coast of South America, provided some preliminary data on latitude effects on the ozone distribution.

In 1967, six distributions were obtained over Barking Sands, Hawaii, (Reference 10) for comparison with ozone profiles inferred from ultraviolet earth-radiance measurements taken with the OGO-4 satellite (Reference 11). In 1968, soundings were made from Fort Churchill, Manitoba, to examine hemispheric differences at high latitudes; and from Wallops Island, Virginia, for comparison with a rocket-borne chemiluminescent ozone sensor (Reference 12). Early in 1969, two soundings were made from Wallops Island to examine possible relationships with a D-region Winter Anomaly. Since 1970, the instrument has been flown for comparison of results with the Backscatter Ultraviolet experiment on the Nimbus-4 satellite (Reference 13).

Twenty-one flights have been selected for this study. Six other soundings have not been included because final results are not available or because data exist only for a limited height range. The launch dates and the locations and geographic coordinates of the launch sites for the selected soundings are listed in Table 1. These soundings were made at latitudes from 58° S to 64° N and longitudes from 75° W to 160° W. Except for low latitudes in the southern hemisphere and extreme polar latitudes, data are available for most climatic zones.

The results do not provide a uniform representation of all seasons, although flights were made in every month of the year except May and December. The largest number of soundings (ten) comes from the fall season in both hemispheres. Five soundings were made in summer, five more in winter, and the single flight made in spring was launched near the equator. Therefore the

Table 1

Rocket Flight Used in Analysis

Flight Number and Date	Location	Launch Site
1. Mar. 7, 1965	4° N, 82° W	Shipboard
2. Apr. 10, 1965	47° S, 78° W	"
3. Apr. 11, 1965	52° S, 78° W	"
4. Apr. 12, 1965	58° S, 78° W	"
5. Sept. 17, 1967	22° N, 160° W	Barking Sands, Hawaii
6. Sept. 20, 1967	"	" " "
7. Oct. 13, 1967	"	" " "
8. Oct. 19, 1967	"	" " "
9. Oct. 22, 1967	"	" " "
10. Oct. 25, 1967	"	" " "
11. July 19, 1968	59° N, 94° W	Fort Churchill, Man.
12. Sept. 16, 1968	38° N, 75° W	Wallops Island, Va.
13. Jan. 31, 1969	"	" " "
14. Feb. 6, 1969	"	" " "
15. June 18, 1970	34° N, 119° W	Point Mugu, Calif.
16. Oct. 17, 1970	55° N, 110° W	Primrose Lake, Alta.
17. Nov. 6, 1970	9° N, 80° W	Fort Sherman, C.Z.
18. Nov. 13, 1970	"	" " "
19. Feb. 24, 1971	22° N, 160° W	Barking Sands, Hawaii
20. Mar. 3, 1971	"	" " "
21. Aug. 14, 1971	64° N, 146° W	Fort Greely, Alaska

statistical data derived from these soundings should not be construed as representing annual mean conditions.

The greatest number of soundings at a single location is eight, at Barking Sands, Hawaii. This large number is due principally to a concentrated effort for satellite comparisons in 1967.

Although diurnal changes in the ozone density are not believed to exist at altitudes below 50 km, it should be noted that our rocket flights have been made within three hours of local noon. The densities are representative of noontime conditions.

It should also be noted that during the years 1967-1969, anomalous absorption of light in the range from 2900 to 3050 Angstroms was found at altitudes above 50 km (References 14 and 15). It is believed that the ozone results are not seriously contaminated by this extraneous absorption. However, an increased variability found at altitudes below 35 km may be due to effects on data from an instrument channel centered at a wavelength near the edge of this absorption band. In 1968, this particular channel was shifted to a wavelength which seemed to be less subject to spectral bias by the absorption. The anomalous absorption was not observed after 1969.

A tabulation of the ozone densities in molecules/cm³ for each of the 21 flights is given in Table 2. The flight numbers correspond to the numbers in Table 1. Complete results for the soundings from 1965 to 1970 are published elsewhere (Reference 16).

Mean Ozone Densities

The mean ozone densities for the 21 soundings have been computed at each even kilometer level from 20 to 52 km. These mean values in molecules/cm³, the associated standard deviations, and the percentage variability that the standard deviation represents are tabulated versus geometric height in kilometers in Table 3. In addition, the maximum and minimum observed densities are shown for each level and an identification number corresponding to the number of the sounding given in Table 1 which produced the extreme value is given.

In Figure 1, the mean ozone densities have been plotted as small circles at even kilometer levels connected with a bold line. Horizontal bars through the circles show the range of values found in these rocket flights. It will be noted by examination of Table 2 that the minima and maxima are not associated

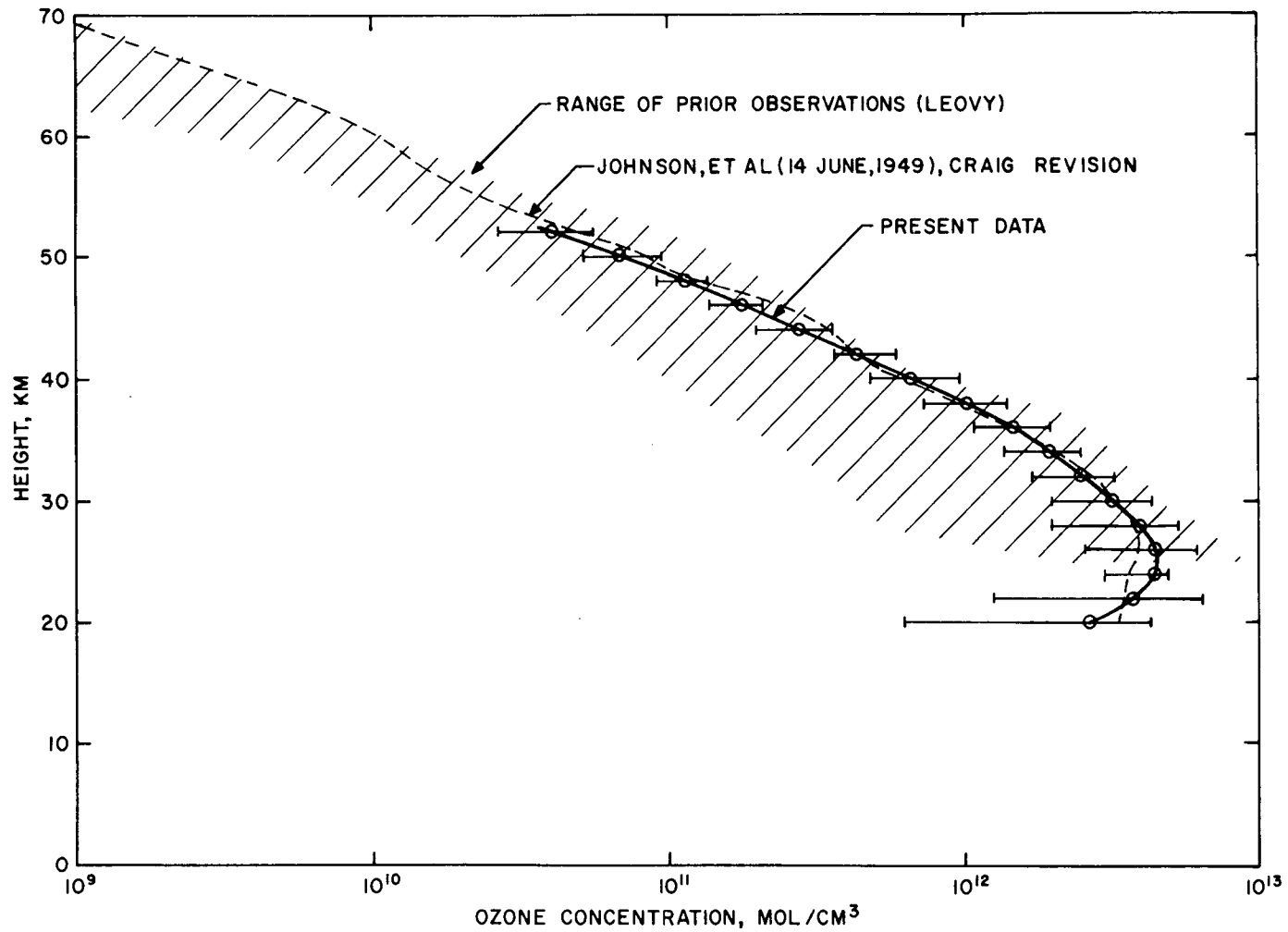


Figure 1. The Mean Ozone Densities from 21 Rocket Flights (Bold Line) Compared with the Data from Johnson et al. as Revised by Craig (Reference 3). The Range of Observations in the Present Data (Shown by the Bars at Each Height Level) Is Compared with a Summary of Earlier Data by Leovy (Reference 17) as Shown by the Crosshatched Area.

Table 2
Ozone Densities (molecules/cm³) Versus Height for the Rocket Flights of Table 1

Sounding No.	1	2	3	4	5	6	7	8	9	10	11
Height (km)											
20	1.1×10^{12}	4.0×10^{12}	6.3×10^{12}	3.6×10^{12}	---	2.0×10^{12}	2.2×10^{12}	---	---	---	---
22	1.7×10^{12}	4.7×10^{12}	6.4×10^{12}	4.4×10^{12}	3.1×10^{12}	3.7×10^{12}	3.7×10^{12}	1.2×10^{12}	2.8×10^{12}	1.9×10^{12}	---
24	3.0×10^{12}	4.7×10^{12}	5.8×10^{12}	4.8×10^{12}	4.9×10^{12}	4.4×10^{12}	4.5×10^{12}	3.8×10^{12}	5.1×10^{12}	3.6×10^{12}	---
26	4.2×10^{12}	4.0×10^{12}	3.4×10^{12}	3.4×10^{12}	5.3×10^{12}	5.2×10^{12}	5.2×10^{12}	4.0×10^{12}	5.6×10^{12}	4.0×10^{12}	---
28	4.5×10^{12}	2.8×10^{12}	3.1×10^{12}	2.5×10^{12}	5.0×10^{12}	5.1×10^{12}	4.5×10^{12}	3.2×10^{12}	5.4×10^{12}	4.0×10^{12}	---
30	4.4×10^{12}	2.4×10^{12}	2.4×10^{12}	2.1×10^{12}	3.9×10^{12}	3.9×10^{12}	4.0×10^{12}	3.1×10^{12}	4.2×10^{12}	3.3×10^{12}	2.6×10^{12}
32	3.2×10^{12}	2.3×10^{12}	1.8×10^{12}	1.7×10^{12}	3.1×10^{12}	3.1×10^{12}	3.1×10^{12}	2.9×10^{12}	3.1×10^{12}	2.8×10^{12}	2.0×10^{12}
34	2.1×10^{12}	1.8×10^{12}	1.4×10^{12}	1.4×10^{12}	2.2×10^{12}	2.5×10^{12}	2.2×10^{12}	2.3×10^{12}	2.3×10^{12}	2.2×10^{12}	1.6×10^{12}
36	1.3×10^{12}	1.5×10^{12}	1.2×10^{12}	1.1×10^{12}	1.5×10^{12}	1.9×10^{12}	1.6×10^{12}	1.4×10^{12}	1.8×10^{12}	1.6×10^{12}	1.1×10^{12}
38	8.3×10^{11}	1.1×10^{12}	9.5×10^{11}	7.8×10^{11}	1.4×10^{12}	1.1×10^{12}	1.2×10^{12}	1.1×10^{12}	8.9×10^{11}	1.2×10^{12}	8.7×10^{11}
40	5.4×10^{11}	8.1×10^{11}	7.1×10^{11}	5.3×10^{11}	9.7×10^{11}	8.4×10^{11}	6.8×10^{11}	6.7×10^{11}	6.5×10^{11}	7.8×10^{11}	6.6×10^{11}
42	3.6×10^{11}	5.9×10^{11}	5.0×10^{11}	4.0×10^{11}	4.3×10^{11}	4.4×10^{11}	4.6×10^{11}	5.1×10^{11}	4.1×10^{11}	4.7×10^{11}	3.7×10^{11}
44	2.4×10^{11}	3.6×10^{11}	2.8×10^{11}	2.7×10^{11}	2.6×10^{11}	2.7×10^{11}	2.4×10^{11}	3.1×10^{11}	2.4×10^{11}	2.6×10^{11}	2.5×10^{11}
46	1.5×10^{11}	---	---	1.8×10^{11}	1.7×10^{11}	1.4×10^{11}	1.5×10^{11}	1.5×10^{11}	1.5×10^{11}	1.6×10^{11}	1.7×10^{11}
48	1.0×10^{11}	---	---	---	1.1×10^{11}	9.1×10^{10}	1.0×10^{11}	1.1×10^{11}	9.1×10^{10}	1.2×10^{11}	1.3×10^{11}
50	6.4×10^{10}	---	---	---	7.3×10^{10}	---	6.4×10^{10}	8.6×10^{10}	5.1×10^{10}	6.7×10^{10}	8.3×10^{10}
52	4.3×10^{10}	---	---	---	5.1×10^{10}	---	---	5.6×10^{10}	3.0×10^{10}	---	4.6×10^{10}

Table 2
Ozone Densities (molecules/cm³) Versus Height for the Rocket Flights of Table 1 (Continued)

Sounding No.	12	13	14	15	16	17	18	19	20	21
Height (km)										
20	3.4×10^{12}	3.2×10^{12}	5.0×10^{12}	---	2.2×10^{12}	1.6×10^{12}	1.9×10^{12}	---	3.3×10^{12}	3.8×10^{12}
22	3.9×10^{12}	4.8×10^{12}	5.8×10^{12}	4.6×10^{12}	3.7×10^{12}	3.6×10^{12}	4.4×10^{12}	4.5×10^{12}	4.3×10^{12}	3.5×10^{12}
24	4.2×10^{12}	5.9×10^{12}	5.7×10^{12}	4.8×10^{12}	4.4×10^{12}	4.5×10^{12}	5.0×10^{12}	4.2×10^{12}	4.3×10^{12}	3.1×10^{12}
26	4.6×10^{12}	4.2×10^{12}	5.0×10^{12}	5.4×10^{12}	6.2×10^{12}	3.9×10^{12}	4.7×10^{12}	4.0×10^{12}	4.3×10^{12}	2.6×10^{12}
28	3.6×10^{12}	3.0×10^{12}	3.8×10^{12}	4.8×10^{12}	4.1×10^{12}	4.7×10^{12}	4.5×10^{12}	3.2×10^{12}	3.6×10^{12}	2.0×10^{12}
30	2.8×10^{12}	2.6×10^{12}	2.8×10^{12}	3.6×10^{12}	2.3×10^{12}	3.2×10^{12}	3.6×10^{12}	2.8×10^{12}	3.0×10^{12}	2.0×10^{12}
32	2.1×10^{12}	2.1×10^{12}	2.0×10^{12}	3.2×10^{12}	2.0×10^{12}	2.5×10^{12}	2.2×10^{12}	2.2×10^{12}	2.6×10^{12}	1.7×10^{12}
34	1.8×10^{12}	1.5×10^{12}	1.4×10^{12}	2.2×10^{12}	1.6×10^{12}	1.9×10^{12}	1.5×10^{12}	1.9×10^{12}	1.9×10^{12}	1.5×10^{12}
36	1.3×10^{12}	1.2×10^{12}	1.2×10^{12}	1.6×10^{12}	1.3×10^{12}	1.3×10^{12}	1.1×10^{12}	1.2×10^{12}	1.4×10^{12}	1.2×10^{12}
38	9.9×10^{11}	7.2×10^{11}	7.7×10^{11}	1.1×10^{12}	8.3×10^{11}	8.2×10^{11}	8.8×10^{11}	8.5×10^{11}	9.8×10^{11}	8.8×10^{11}
40	7.1×10^{11}	5.1×10^{11}	4.8×10^{11}	7.4×10^{11}	6.3×10^{11}	7.1×10^{11}	6.3×10^{11}	5.9×10^{11}	6.6×10^{11}	---
42	4.8×10^{11}	3.6×10^{11}	3.7×10^{11}	4.6×10^{11}	3.6×10^{11}	5.4×10^{11}	3.6×10^{11}	3.9×10^{11}	4.2×10^{11}	---
44	2.9×10^{11}	2.4×10^{11}	2.4×10^{11}	2.9×10^{11}	3.6×10^{11}	2.9×10^{11}	2.3×10^{11}	2.0×10^{11}	2.7×10^{11}	---
46	1.5×10^{11}	---	1.6×10^{11}	1.9×10^{11}	2.1×10^{11}	1.9×10^{11}	1.4×10^{11}	1.4×10^{11}	2.1×10^{11}	---
48	1.0×10^{11}	---	1.0×10^{11}	1.2×10^{11}	1.1×10^{11}	1.3×10^{11}	---	9.4×10^{10}	1.3×10^{11}	---
50	7.3×10^{10}	---	---	7.5×10^{10}	6.7×10^{10}	8.3×10^{10}	---	7.0×10^{10}	9.4×10^{10}	---
52	---	---	---	---	---	5.1×10^{10}	---	---	---	---

Table 3
Results of Rocket Soundings

Height (km)	Ozone Density (molecules/cm ³)	Standard Deviation	Percent Variability	Maximum Observed Density	Number of Sounding (see Table 1)	Minimum Observed Density	Number of Sounding (see Table 1)
20	3.11×10^{12}	1.42×10^{12}	45 %	6.34×10^{12}	3	1.07×10^{12}	1
22	3.82×10^{12}	1.28×10^{12}	33 %	6.42×10^{12}	3	1.24×10^{12}	8
24	4.49×10^{12}	0.74×10^{12}	17 %	5.83×10^{12}	3	2.98×10^{12}	1
26	4.43×10^{12}	0.86×10^{12}	19 %	6.15×10^{12}	16	2.55×10^{12}	21
28	3.87×10^{12}	0.94×10^{12}	24 %	5.35×10^{12}	9	1.97×10^{12}	21
30	3.10×10^{12}	0.70×10^{12}	22 %	4.35×10^{12}	1	1.95×10^{12}	21
32	2.46×10^{12}	0.53×10^{12}	21 %	3.22×10^{12}	1	1.67×10^{12}	4
34	1.86×10^{12}	0.35×10^{12}	19 %	2.47×10^{12}	6	1.35×10^{12}	14
36	1.37×10^{12}	0.23×10^{12}	16 %	1.93×10^{12}	6	1.07×10^{12}	4
38	9.57×10^{11}	1.67×10^{11}	17 %	14.0×10^{11}	5	7.23×10^{11}	13
40	6.72×10^{11}	1.18×10^{11}	18 %	9.68×10^{11}	5	4.81×10^{11}	14
42	4.33×10^{11}	0.64×10^{11}	15 %	5.86×10^{11}	2	3.57×10^{11}	18
44	2.69×10^{11}	0.40×10^{11}	15 %	3.60×10^{11}	2	2.00×10^{11}	19
46	1.66×10^{11}	0.24×10^{11}	14 %	2.12×10^{11}	16	1.37×10^{11}	18
48	1.10×10^{11}	0.13×10^{11}	12 %	1.34×10^{11}	17	0.91×10^{11}	9
50	7.00×10^{10}	1.10×10^{10}	15 %	9.41×10^{10}	20	5.11×10^{10}	9
52	4.00×10^{10}	1.10×10^{10}	27 %	5.60×10^{10}	8	2.70×10^{10}	16

with any individual soundings. Instead, these extremes result from rather subtle variations in the shape of the distribution. Below 35 km, the maxima arise from a shift of the ozone density maximum to lower altitudes with increasing latitude. Above 40 km, the lowest values tend to come from the low latitudes. The character of these latitude effects is not readily apparent in a density diagram. Mixing-ratio profiles derived from the densities, on the other hand, show systematic changes from low to high latitudes. These variations will be discussed in a separate publication.

Variabilities

The percentage variability listed in Table 2 shows a tendency to decrease with altitude above 28 km, with the lowest value, 12 percent, found at 48 km. The increase at 50 and 52 km is likely not real, but rather an artifact of endpoint data near the tops of the soundings.

In Figure 1, these results have been compared with other measurements. The data from the Johnson, Purcell, Tousey, and Watanabe sounding of June 14, 1949, as revised by Craig (Reference 3) are shown as the dashed line. It is clear that, except for the value at 46 km, no disagreement exists. The present data have also been compared with a compilation of prior observations by Leovy (Reference 17), which is shown by the crosshatched area. The range of ozone densities given by these earlier balloon, rocket, and satellite observations is believed to be an overestimate of the natural variability of stratospheric ozone. The ozone density range at each height found in the present study is approximately ± 30 percent of the mean value at 50 km; ± 40 percent at 40 km; ± 40 percent at 30 km; and $+200$ percent, -66 percent at 20 km for the summer, fall, and winter seasons.

ACKNOWLEDGEMENTS

The support for these flights by the Geophysics Division, Pacific Missile Range, Point Mugu, California; the 6th Weather Wing, Andrews Air Force Base, Maryland; the Atmospheric Sciences Laboratory, U.S. Army Electronics Command, White Sands Missile Range, New Mexico; the 448th Test Sq., Canadian Forces Base, Cold Lake, Alberta; and many individuals including Dr. W. R. McBride and W. L. Burson, Naval Weapons Center, China Lake, California; P. G. Simeth and C. S. Cramer, formerly of Metrophysics, Inc., Santa Barbara, California, is gratefully acknowledged.

REFERENCES

1. E. Regener and V. H. Regener. "Aufnahme des ultravioletten Sonnenspektrums in der Stratosphäre und vertikale Ozonverteilung." *Physik. Z* (1934), 32. pp. 121 ff.
2. F. S. Johnson, J. D. Purcell, R. Tousey, and K. Watanabe. "Direct Measurements of the Vertical Distribution of Atmospheric Ozone to 70 Kilometers Altitude. *J. Geophys. Res.*, 57, (1952). pp. 157-76.
3. R. A. Craig. *The Upper Atmosphere: Meteorology and Physics*. New York, 1965. p. 194.
4. W. Kulcke and H. K. Paetzold. "Über eine Radiosonde zur bestimmung der vertikalen Ozonverteilung." *Ann. d. Met.*, 8 (1957). pp. 47 ff.
5. A. Vassy. "Atmospheric Ozone." *Advances in Geophysics*, 11 (1965). pp. 115-73.
6. J. Kobayashi, M. Kyojuka, and H. Muramatsu. "On Various Methods of Measuring the Vertical Distribution of Atmospheric Ozone (I) — Optical Type Ozone-sonde." *Papers Meteorol. Geophys.*, 17 (1966). pp. 76-96.
7. A. J. Krueger and W. R. McBride. "Rocket Ozone-sonde (ROCOZ) — Design and Development." *Naval Weapons Center Technical Publication* 4512. 1968.
8. E. C. Y. Inn and Y. Tanaka. "Ozone Absorption Coefficients in the Visible and Ultraviolet Regions." *Adv. in Chem. Series* 21 (1959). pp. 263-268. American Chemical Society, Washington, D.C.
9. E. Vigroux. "Contribution a l'etude experimentale de l'absorption de l'ozone." *Ann. Phys.*, 8 (1953). pp. 709-62.
10. A. J. Krueger. "Rocket Measurements of Ozone Over Hawaii." *Ann. Geophys.*, 25 (1969). pp. 307-11.
11. G. P. Anderson, C. A. Barth, F. Cayla, and J. London. "Satellite Observations of the Vertical Ozone Distribution in the Upper Stratosphere." *Ann. Geophys.*, 25 (1969). pp. 239-43.

12. E. Hilsenrath, L. Seiden, and P. Goodman. "An Ozone Measurement in the Mesosphere and Stratosphere by Means of a Rocketsonde." J. Geophys. Res., 71 (1969). pp. 1385-97.
13. A. J. Krueger, D. F. Heath, and C. L. Mateer. "Variations in the Stratospheric Ozone Field Inferred from Nimbus Satellite Observations." Pure and Applied Geophysics (1973). In press.
14. A. J. Krueger. "Atmospheric Absorption Anomalies in the Ultraviolet Near an Altitude of 50 Kilometers." Science, 166 (1969). pp. 998-1000.
15. T. Nagata, T. Tohmatsu, and T. Ogawa. "Sounding Rocket Measurement of Atmospheric Ozone Density, 1965-1970." Space Research XI 1971. pp. 849-55.
16. A. J. Krueger. "Rocket Soundings of Ozone: ROCOZ-Arcas Results 1965-1970. In preparation.
17. C. B. Leovy. "Atmospheric Ozone: An Analytic Model for Photochemistry in the Presence of Water Vapor." J. Geophys. Res., 74, 1969. pp. 417-26.